

Supplementary Information

for

**Switching p-type to high-performance n-type organic electrochemical transistors
via doped state engineering**

Peiyun Li^{1, #}, Junwei Shi^{1,2, #}, Yuqiu Lei³, Zhen Huang², and Ting Lei^{1,}*

¹Key Laboratory of Polymer Chemistry and Physics of Ministry of Education, Shool of Materials Science and Engineering, Peking University, Beijing 100871, China

²College of Chemistry and Molecular Engineering, Peking University, Beijing 100871, China.

³College of Engineering, Peking University, Beijing 100871, China

[#]These authors contributed equally to this work

*E-mail: tinglei@pku.edu.cn

Table of Contents

1. Experimental Details

2. Supplementary Tables and Figures

3. Synthesis and Characterization of New Compounds

4. References

1. Experimental Details

Materials

All the chemical reagents were purchased and used as received unless otherwise indicated. All air and water-sensitive reactions were performed under a nitrogen atmosphere. Dichloromethane (DCM), Tetrahydrofuran (THF), Toluene, and *N*, *N*-Dimethylformamide (DMF) were dried by a JC Meyer solvent drying system before use. Ultradry solvents were obtained from J&K reagent company.

Chemical structure and optoelectronic property characterization

¹H NMR and ¹³C NMR spectra were recorded on Bruker ARX-400 (400 MHz). All chemical shifts were reported in parts per million (ppm). ¹H NMR chemical shifts were referenced to CDCl₃ (7.26 ppm), and ¹³C NMR chemical shifts were referenced to CDCl₃ (77.16 ppm). Mass spectra were recorded on an FTMS Fourier transform high-resolution mass spectrometer. Thermal gravity analyses (TGA) were carried out on a TA Instrument Q600 SDT analyzer, and differential scanning calorimetry (DSC) analyses were performed on a TA Instrument Q2000 analyzer. Absorption spectra were recorded on PerkinElmer Lambda 750 UV-vis spectrometer. Cyclic voltammograms (CV) were measured through an electrochemical workstation SP-300 (BioLogic Science Instruments). A standard three-electrode setup was established by employing polymer-coated ITO glass slides as the working electrode (WE), a block of platinum mesh as the counter electrode (CE), and an AgCl/Ag pellet (Warner Instruments) as the reference electrode (RE), further calibrated against ferrocene (Fc/Fc⁺). The measurements were carried out in an aqueous solution with 0.1 M NaCl or in acetonitrile with 0.1 M tetrabutylammonium hexafluorophosphate as the supporting electrolyte with a scan rate of 50 mV/s. Ionization potentials and electron affinity were obtained using the equation: IP = (E_{Ox} - E_{Fc/Fc⁺} + 4.8) eV, EA = (E_{Red} - E_{Fc/Fc⁺} + 4.8) eV.

Size exclusion chromatography measurement

Polymer number-average molecular weight (M_n) and molecular weight distributions ($PDI = M_w/M_n$) were measured by size exclusion chromatography (SEC). HFIP SEC analyses were performed on a Waters 1515 instrument equipped with a PLMIXED 7.5 \times 50 mm guard column, two PLMIXED-C 7.5 \times 300 columns, and a differential refractive index detector at 35 °C with a flow rate of 1 ml min⁻¹. The instrument was calibrated with 10 PS standards, and chromatograms were processed with Waters Breeze software.

AFM and GIWAXS characterization

Atomic force microscopy (AFM) measurements were performed with Dimension icon ScanAsyst (Bruker). Two-dimensional grazing incidence wide-angle X-ray scattering(2D-GIWAXS) measurements were conducted on a Xenocs-SAXS/WAXS system with an X-ray wavelength of 1.5418 Å and 0.2° as an incidence angle. Pilatus 300 K was used as a 2D detector. Data processing was performed in Igor Pro software with Nika and WAXTools packages.

Spectroelectrochemistry

Spectroelectrochemistry was performed with an ITO-coated glass slide, spun cast with the polymer solution (3×10^{-3} M chloroform solution) at a rotating speed of 500 rpm for 45 s. These polymer-coated ITO slides were employed as the WE and immersed into the cuvette filled with 0.1 M aqueous NaCl solution, followed by the use of Pt mesh (CE) and AgCl/Ag pellet (RE). A PerkinElmer Lambda 750 UV-vis spectrometer was used with the beam path passing through the electrolyte-filled cuvette and polymer-coated ITO samples. A background spectrum with cuvette/electrolyte/ITO was recorded before a potential was applied to the cell. The potential was applied to the WE for 5 s before the spectra were recorded and lasted for a certain amount of time until the completion of spectrum scanning.

OECT fabrication and characterization

The OECTs fabrication included the deposition and patterning of the metallic electrodes, the parylene layer, and the polymer in the channel. In detail, silica substrates were thoroughly cleaned by ultrasonication in acetone, DI water, and isopropyl alcohol, followed by nitrogen blow-drying and brief oxygen plasma cleaning. Metal pad interconnects, and source/drain contacts were patterned. 5 nm Cr and 35 nm Au were subsequently deposited, and then a lift-off process was carried out. Metal interconnects and pads were insulated by depositing 1 μm of parylene-C using a PDS 2010 Labcoater-2, with a 3-(trimethoxysilyl)propyl methacrylate (A-174 Silane) adhesion promoter. A 2% aqueous solution of industrial cleaner (Micro-90) was subsequently spun coated to act as an anti-adhesive for a second sacrificial 1 μm parylene-C film, which was used to simultaneously define the active channel area, and to pattern the underlying parylene layer. Samples were subsequently patterned with a 5 μm thick layer of AZ9260 photoresist and AZ-400K developer. The patterned areas were opened by reactive ion etching with O₂ plasma using an LCCP-6A reactive ion etcher (Leuven Instruments). The polymer was dissolved in chlorobenzene at a concentration of 3mg/ml. The polymer solution was spin-cast on the etched devices. After a peeling-off process of the second sacrificial parylene layer, the OECTs were ready for measurement. The device characterization was performed on a probe station using a Keithley 4200 SCS analyzer or Fs-Pro semiconductor parameter analyzer, PDA. AgCl/Ag pellet (Warner Instruments) was employed as the gate electrode and immersed into a 0.1 M NaCl solution, which covers the polymer film in the channel. The thickness of the film was determined in a dry state after testing with a DEKTAK profilometer (Bruker).

Electrochemical impedance spectra

Electrochemical impedance spectra (EIS) were performed on the polymer-coated electrodes using the electrochemical workstation SP-300 (BioLogic Science Instruments). Polymer film covered on the electrodes was patterned as squares with certain areas through the lithography technique. These polymer-coated electrodes with glass substrate were employed as the working electrode and fully covered with a 0.1 M

NaCl solution, followed by the employment of Pt mesh (CE) and AgCl/Agl pellet (RE) to establish a standard three electrodes system. The capacitances of polymers measured on Au electrodes with various sizes were obtained through the potential-EIS method, with setting the DC offset voltage as the maximum achievable doping for each polymer. The AC amplitude of voltage in the form of sine-wave on the WE was set as 10 mV (RMS) and the frequency was scanned from 1Hz to 100 kHz. The as-obtained Bode plots or Nyquist plots were fitted to an equivalent circuit, namely the Randle's circuit $R_s (R_p||C)$, via the software EC-Lab view. The thickness of the film was determined in a dry state after testing with a DEKTAK profilometer (Bruker).

DFT calculations

Geometry optimization, molecular energy level calculation, and relaxed potential energy surface scan were performed at the B3LYP/6-311g(d,p) or wB97XD/6-311g(d,p) level using Gaussian 16 and Gaussian View 6^{1,2}. The computational results were visualized by Multiwfn³ and VMD⁴.

2. Supplementary Tables and Figures

Table S1. Summary of the Energy Levels and Molecular Weights of Polymers

	HOMO^a (eV)	LUMO^a (eV)	IP^b (eV)	EA^b (eV)	E_b^c (eV)	E_g^c (eV)
P(gTDPPT)	−4.92	−3.25	4.86	3.69	1.36	1.17
P(gTDPP2FT)	−5.03	−3.39	5.20	3.86	1.34	1.38

^aFrom DFT calculations. ^bEstimated from the cyclic voltammetry (CV) measurement. ^cEstimated from the UV-Vis-NIR spectra.

Table S2. OECT Device Parameters for the Two Polymers

	W/L	g_m (mS)	d (nm)	V_{th} (V)	V_{GS} (V)	μC* (F/cm V s)
P(gTDPPT)	10	1.18	60.5	−0.60	−0.90	65.1
	10	0.78	60.5	−0.64	−0.86	53.7
	10	0.60	54.2	−0.60	−0.84	46.1
	10	0.20	54.2	−0.64	−0.84	18.5
Average						45.9
P(gTDPP2FT)	10	0.52	60.6	0.64	0.89	34.3
	10	0.54	60.6	0.65	0.89	37.1
	10	0.67	60.6	0.64	0.90	42.5
	10	0.93	60.6	0.62	0.90	54.8
Average						42.2

Table S3. Comparison of the OEET Performances for the OEET Polymers reported in literature.

Polymer	type	HOMO ^a (eV)	LUMO ^a (eV)	μ (cm ² /V s)	μC^* (F/cm V s)	τ_{on} (ms)	Ref
P(C6-T2)	n	-5.6	-4.2	0.00474	1.29	10	⁵
BBL ₁₅₂	n	-6.12	-4.37	0.0404	25.9	0.38	⁶
f-BTI2TEG-FT	n	-5.59	-3.82	0.0299	15.2	272	⁷
P(C-T)	n	-5.53	-4.25	0.069	7.6	NA	⁸
P(N-T)	n	-5.76	-4.48	0.059	4.9	NA	⁸
P(gPzDPP-CT2)	n	-5.72	-4.19	0.019	1.72	3	⁹
P(g7NC10N)	n	-5.12	-4.23	0.012	1.83	NA	¹⁰
f-BTI2g-TVTCN	n	-5.57	-3.81	0.24	41.3	52	¹¹

^aEstimated from the cyclic voltammetry (CV) measurement.

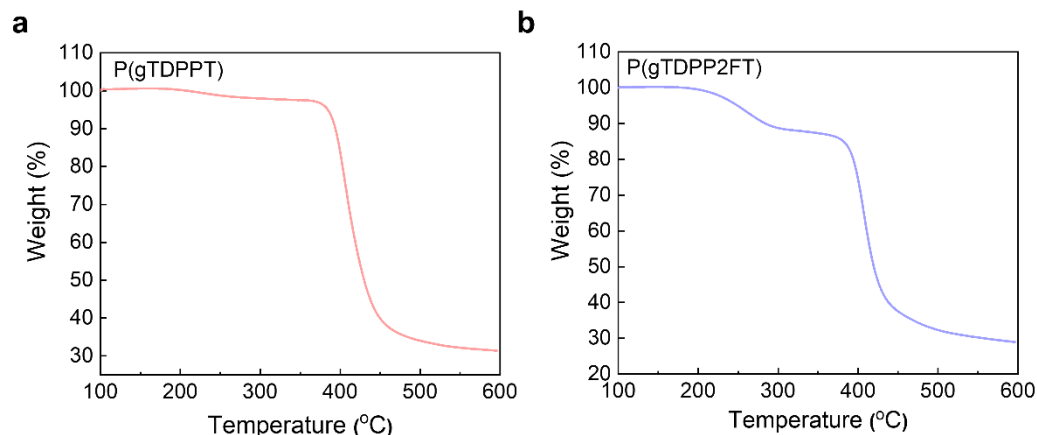


Fig. S1 Thermal gravity analysis (TGA) of **a** P(gTDPPT) and **b** P(gTDPP2FT). Both polymers showed high decomposition temperatures of over 200 °C

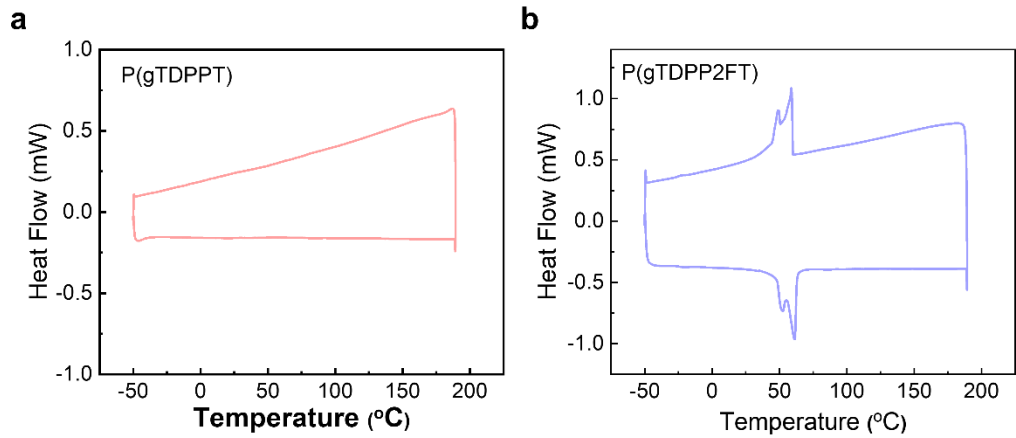


Fig. S2 Differential scanning calorimetry (DSC) of **a** P(gTDPPT) and **b** P(gTDPP2FT).

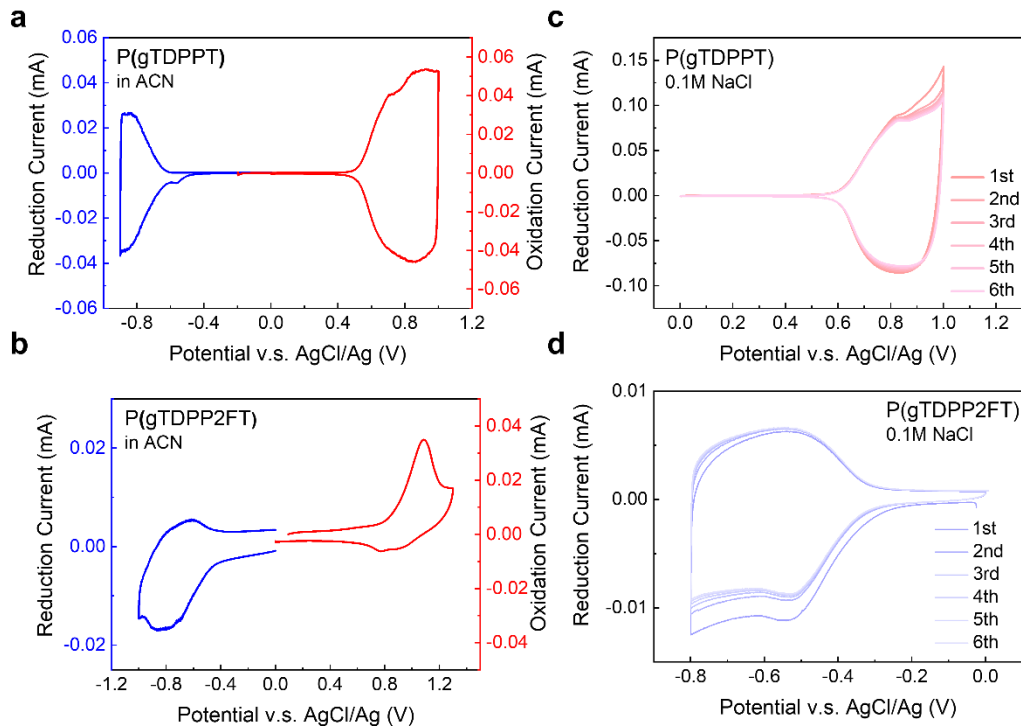


Fig. S3 Cyclic voltammograms of **a** & **c** P(gTDPPT) and **b** & **d** P(gTDPP2FT), in acetonitrile solution with 0.1 M tetrabutylammonium hexafluorophosphate or 0.1 M NaCl as the electrolyte.

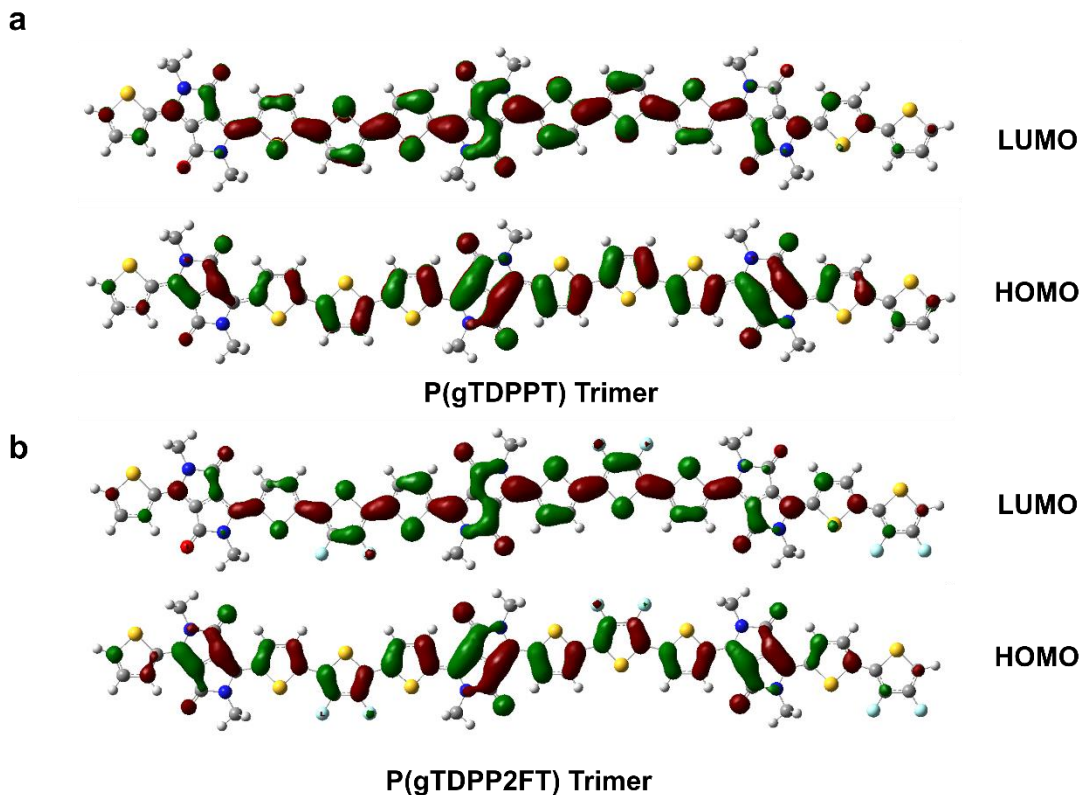


Fig. S4 DFT-optimized geometries and molecular frontier orbitals of the trimers of **a** P(gTDPPT) and **b** P(gTDPP2FT). Calculations were performed at B3LYP/6-311G(d,p) level. Branched glycol side chains were replaced with methyl groups to simplify the calculation.

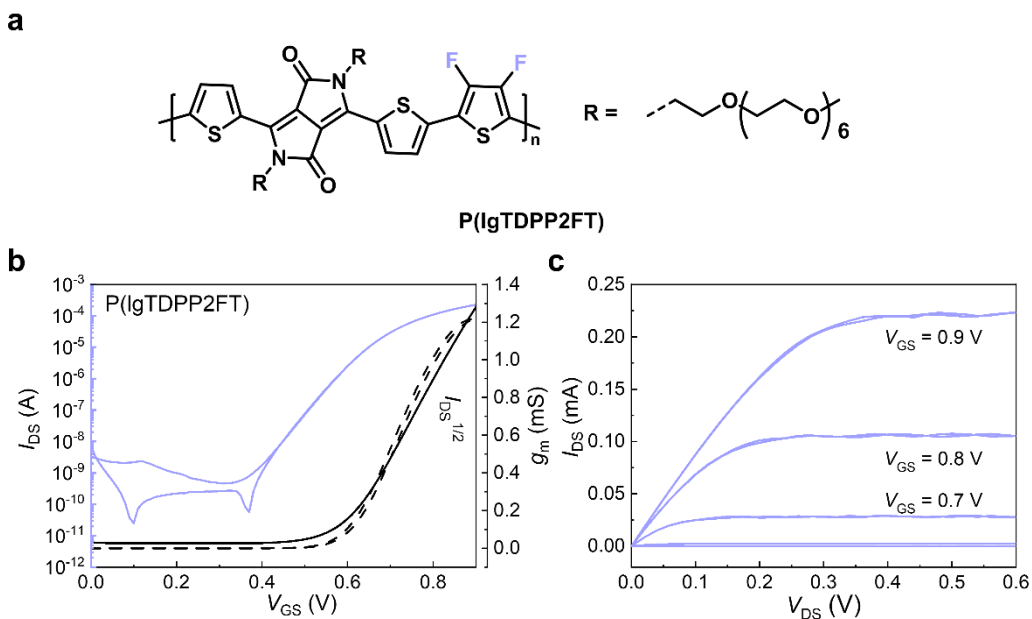


Fig. S5 Chemical structure and OECTs performance of P(lgTDPP2FT). **a** Chemical structure of P(lgTDPP2FT). **b** & **c** Transfer characteristics and output characteristics of P(lgTDPP2FT). $W/L = 100/10 \mu\text{m}$ of all devices and $V_{DS} = 0.6 \text{ V}$ for Fig. b. The μC^* is $20.4 \pm 1.0 \text{ F cm}^{-1} \text{ V}^{-1} \text{ s}^{-1}$.

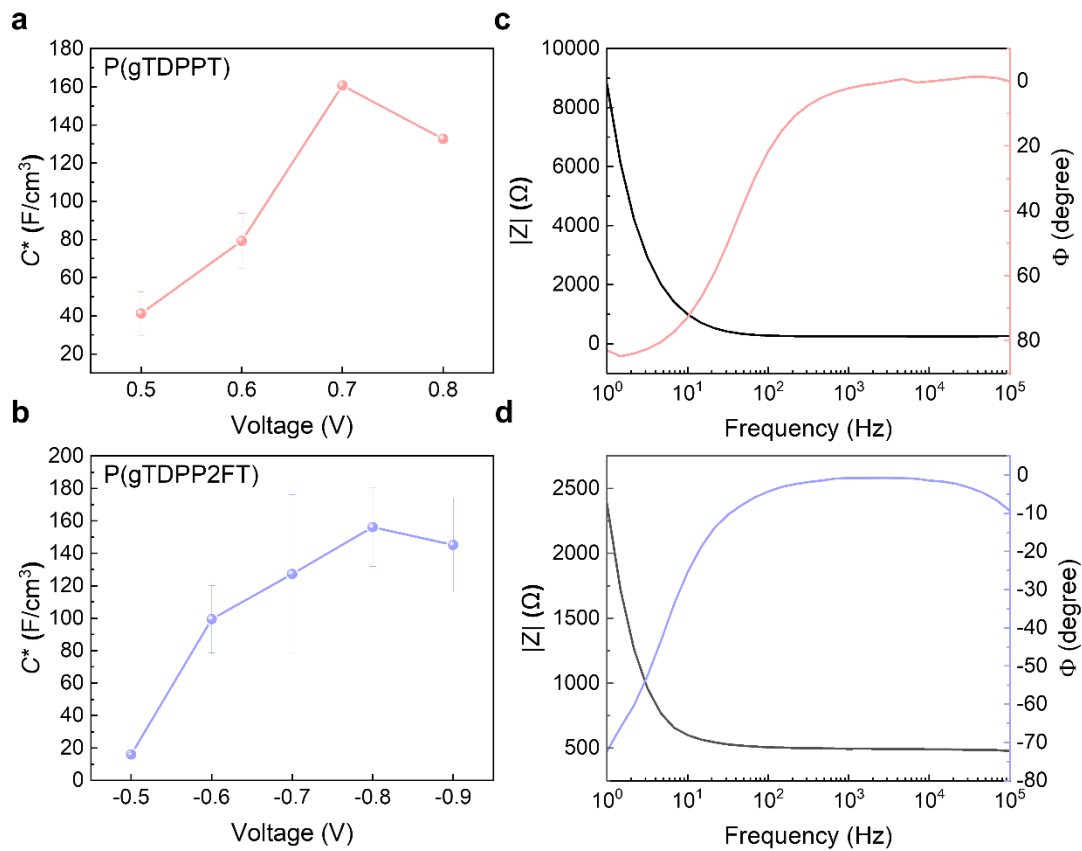


Fig. S6 Capacitive behaviors of both polymers. **a** & **b** Voltage-capacitance relationship of P(gTDPPT) and P(gTDPP2FT) measured through the electrochemical impedance spectrum. **c** & **d** The corresponding Bode and phase plot of P(gTDPPT) and P(gTDPP2FT) with a bias of 0.7 V and -0.8 V, respectively.

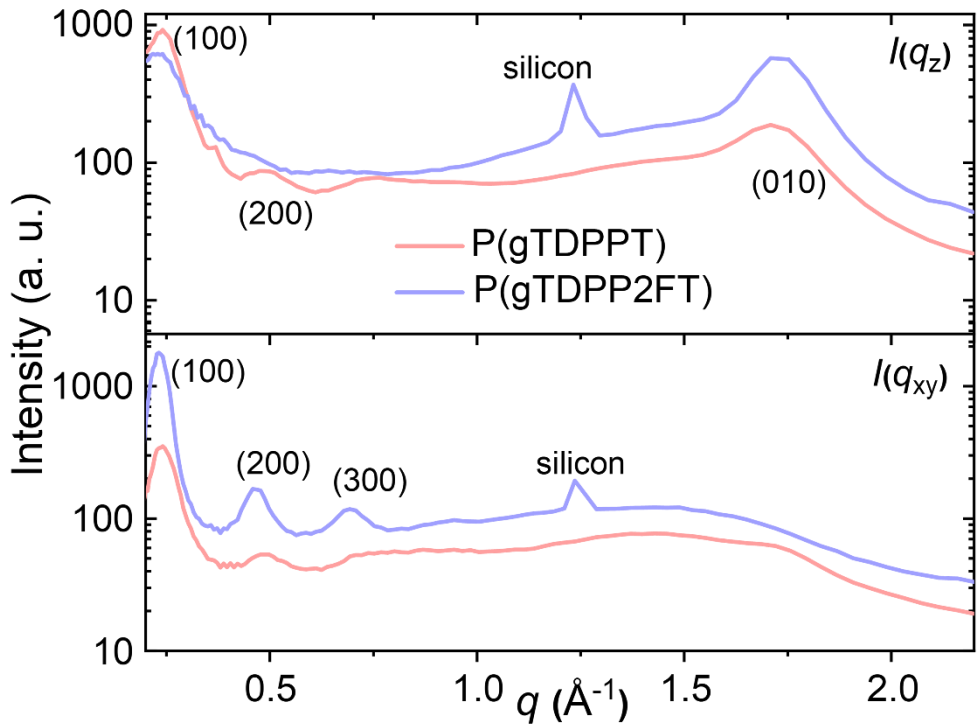


Fig. S7 The corresponding line cuts of the P(gTDPPT) and P(gTDPP2FT) GIWAXS pattern. Cuts along the q_{xy} direction represent scattering in the in-plane direction, while the scattering of the q_z direction results from out-of-plane scattering.

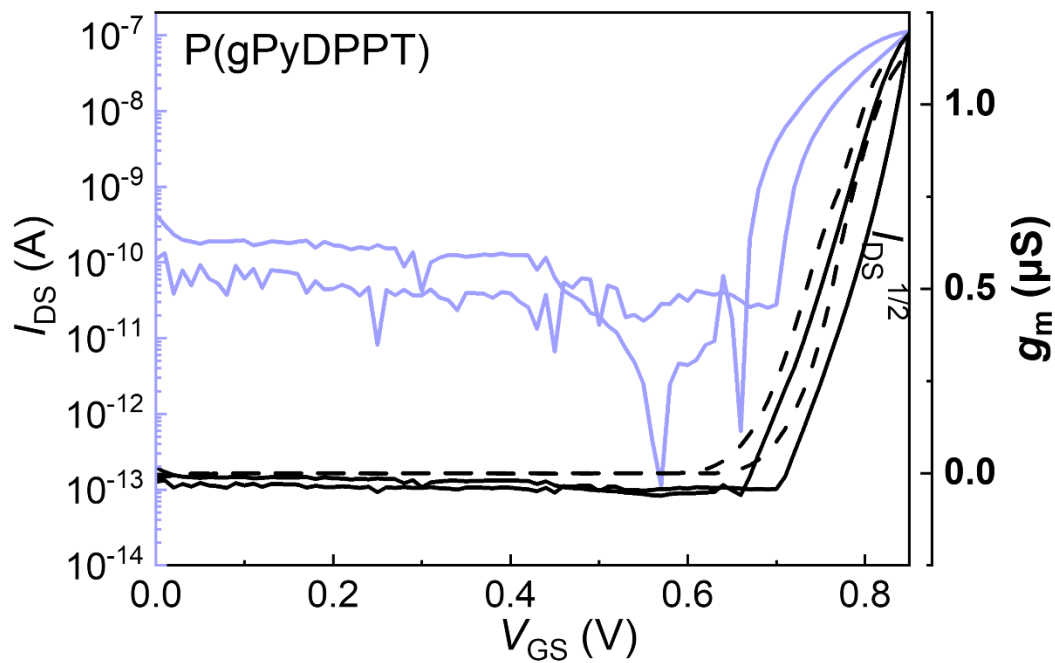


Fig. S8 OECTs performance of P(gPyDPPT). Transfer characteristics of P(gPyDPPT). $W/L =$

100/10 μm and $V_{\text{DS}} = 0.6$ V. The μC^* is $0.07 \text{ F cm}^{-1} \text{ V}^{-1} \text{ s}^{-1}$.

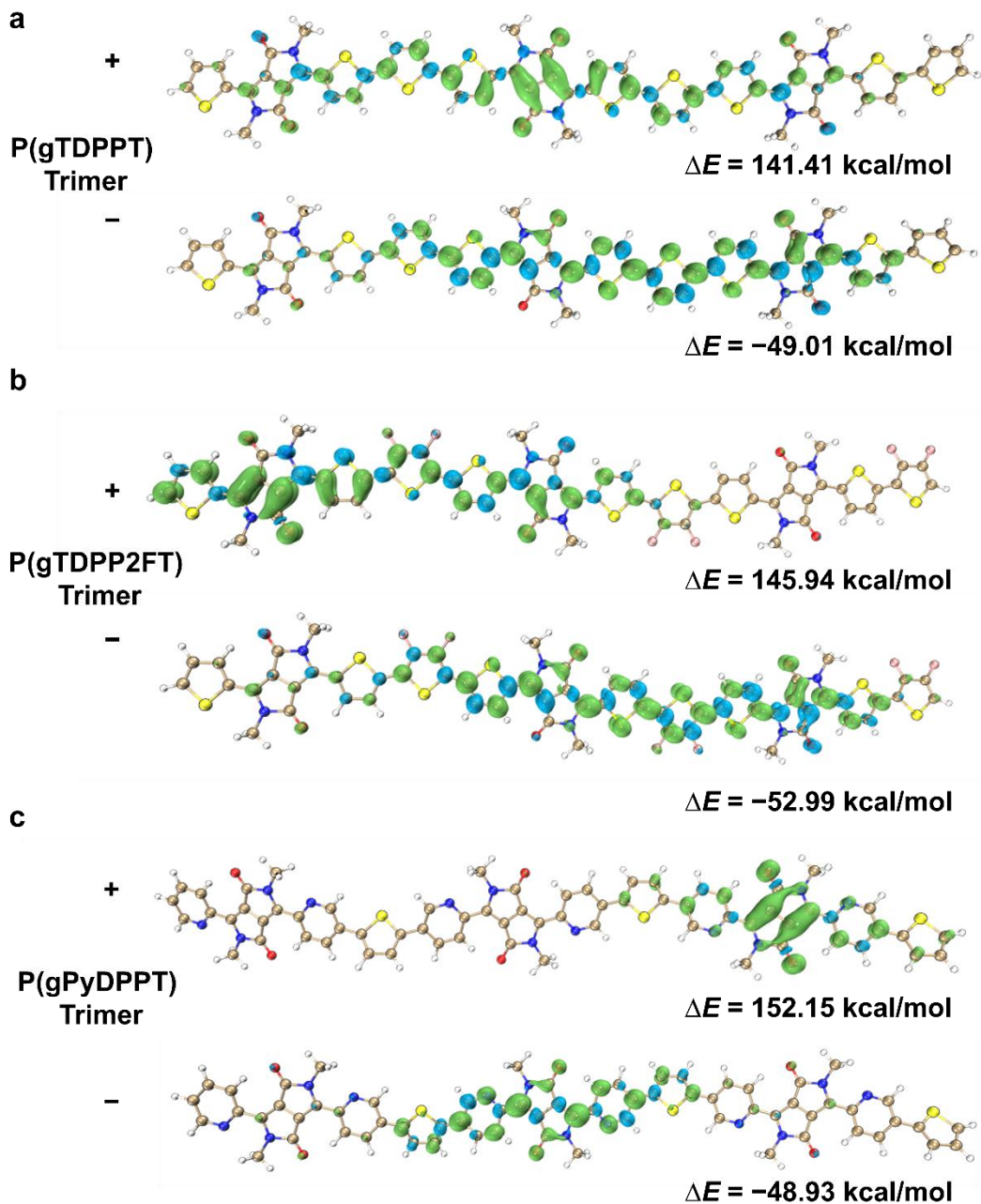


Fig. S9 Spin density distribution of positively (+) or negatively (-) charged for **a** P(gTDPPT), **b** P(gTDPP2FT) and **c** P(gPyDPPT). ΔE stands for the electronic energy change from the neutral to the charged state. There is extra spin density on F atoms of negatively charged P(gTDPP2FT) compared to that of P(gTDPPT). The spin density delocalization length of positively charged P(gTDPPT) is the longest. Both the delocalization length of positively or negatively spin density for P(gPyDPPT) is the shortest.

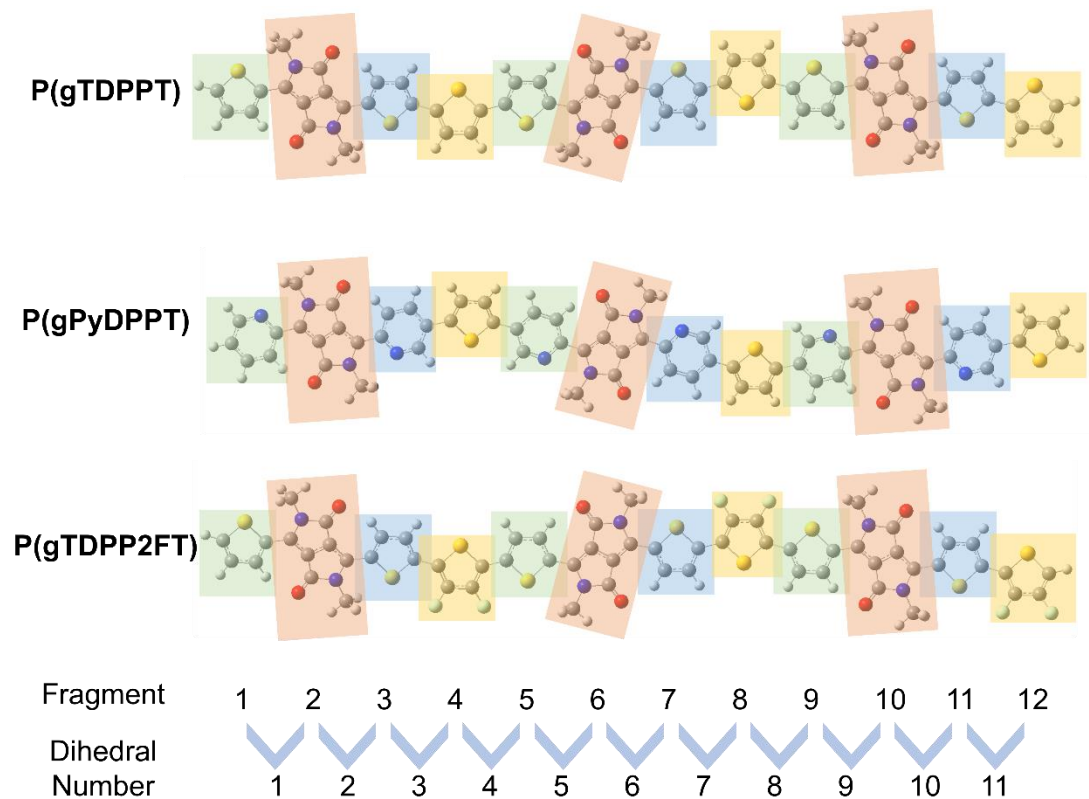
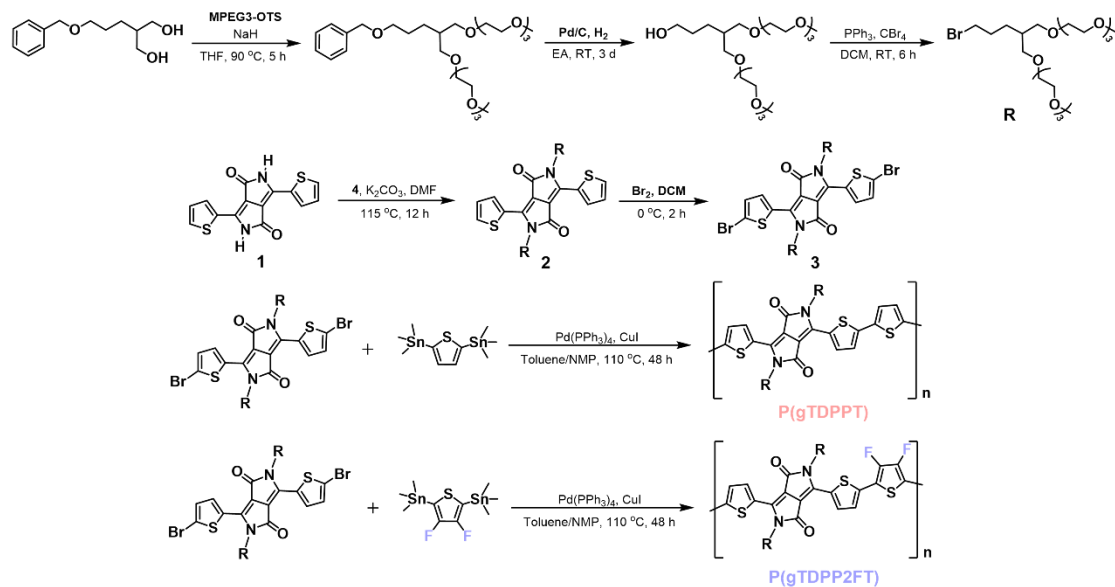


Fig. S10 Schematic diagram of fragment and dihedral numbers for the three polymers.

3. Synthesis and Characterization of New Compounds

Scheme S1. Synthetic routes to the side chain R/monomer 3 and the polymers.



The synthesis of the side chain R follows our previous work⁹.

Synthesis of compound 2

Under nitrogen atmosphere, **1** (500 mg, 1.66 mmol) and potassium carbonate (1.14 g, 8.3 mmol) were added to 15 mL of *N,N*-dimethylformamide. After heating the mixture to 115 °C, **R** (1.6 g, 3.36 mmol) in DMF (5 mL) was added dropwise into the mixture and stirred for 12 h. After cooling to room temperature (RT), the mixture was washed with water and extracted with DCM. The residue was purified by silica gel column chromatography using EA/MeOH (*v:v*, 30/1) as the eluent to get a red solid **2** (350 mg, 31.3%). ¹H NMR (CDCl₃, 400 MHz, TMS), δ (ppm): 8.923-8.911 (d, *J* = 4.8, 2H), 7.681-7.666 (d, *J* = 6, 2 H), 7.301-7.279 (t, *J* = 8.8, 2H), 4.069-4.029 (t, *J* = 16 Hz, 4H), 3.642-3.594 (m, 34H), 3.542-3.527 (m, 16H), 3.423-3.396 (m, 6H), 3.369 (s, 12 H), 1.921-1.891 (m, 2H), 1.786-1.773 (m, 4H), 1.520-1.464 (m, 4H). ¹³C NMR (100 MHz, CDCl₃), δ (ppm): 161.24, 139.92, 135.26, 130.94, 129.72, 128.64, 107.59, 71.93, 71.63, 70.64, 70.60, 70.52, 70.49, 59.04, 42.33, 38.80, 27.43, 25.75.

Synthesis of compound 3

2 (350 mg, 0.314 mmol) was added in 20 mL of DCM. After liquid bromine (102 mg, 0.643 mmol) was added slowly at 0 °C, the mixture was stirred for 2 h. After the reaction was quenched by NaHSO₄ aqueous solution, the mixture was washed with water and extracted with DCM. The residue was purified by silica gel column chromatography using EA/MeOH (*v*:*v*, 40/1) as the eluent to get a red solid **3** (205 mg, 51.25%). ¹H NMR (CDCl₃, 400 MHz, TMS), δ (ppm): 8.660-8.650 (d, *J* = 4, 2H), 7.266-7.256 (d, *J* = 4, 2H), 3.979-3.940 (t, *J* = 15.6, 4H), 3.644-3.601 (m, 34H), 3.565-3.529 (m, 16H), 3.447-3.382 (m, 6H), 3.372 (s, 12 H), 1.921-1.877 (m, 2H), 1.760-1.72 (m, 4H), 1.509-1.453 (m, 4H). ¹³C NMR (100 MHz, CDCl₃), δ (ppm): 159.89, 137.85, 134.28, 130.71, 130.05, 118.16, 106.73, 70.92, 70.63, 69.63, 69.58, 69.51, 69.50, 69.47, 58.03, 41.39, 37.77, 26.49, 24.79. FTMS calcd. for (M + H)⁺: 1274.36633, Found: 1274.40453.

Synthesis of polymer P(gTDPPT)

Tetratriphenylphosphine palladium (0.91 mg, 0.78 μ mol), cuprous iodide (0.29 mg, 1.57 μ mol), 2,5-bis(trimethylstannyl)thiophene (10.71 mg, 26.14 μ mol) and **3** (34 mg, 26.66 μ mol) and toluene/N-methylpyrrolidone (3 mL/3 mL) was added in a 25 mL Schlenk tube. The tube was charged with nitrogen through a freeze-pump-thaw cycle three times. The sealed tube was heated to 110 °C and stirred for 48 h. After cooling the reaction mixture to room temperature, diethylphenylazothioformamide (3 mg) was added to remove the catalyst and the resulting mixture was stirred at 80 °C for 1 h. The reaction mixture was poured into 50 mL hexane to precipitate and filter the polymer. The polymer solid was placed in a Soxhlet extractor and extracted with hexane, methanol, acetone, and chloroform. The chloroform solution was concentrated under reduced pressure and then poured into 20 mL hexane to reprecipitate the polymer P(gTDPPT). The suspension was filtered and dried in vacuum to afford the polymer. The P(gTDPPT) was synthesized according to the literature¹².

Synthesis of polymer P(gTDPP2FT)

Tetratriphenylphosphine palladium (0.9 mg, 0.78 μ mol), cuprous iodide (0.3 mg, 0.84 μ mol), (3,4-difluorothiophene-2,5-diyl)bis(trimethylstannane) (11.58 mg, 25.98 μ mol) and **3** (34.12 mg, 26.76 μ mol) and toluene/N-methylpyrrolidone (3 mL/3 mL) was added in a 25 mL Schlenk tube. The tube was charged with nitrogen through a freeze-pump-thaw cycle three times. The sealed tube was heated to 110 °C and stirred for 48 h. After cooling the reaction mixture to room temperature, diethylphenylazothioformamide (3 mg) was added to remove the catalyst and the resulting mixture was stirred at 80 °C for 1 h. The reaction mixture was poured into 50 mL hexane to precipitate and filter the polymer. The polymer solid was placed in a Soxhlet extractor and extracted with hexane, methanol, acetone, and chloroform. The chloroform solution was concentrated under reduced pressure and then poured into 20 mL hexane to reprecipitate the polymer P(gTDPP2FT). The suspension was filtered and dried in vacuum to afford the polymer. M_n : 30.7 kDa; M_w : 65.0 kDa; PDI: 2.1.

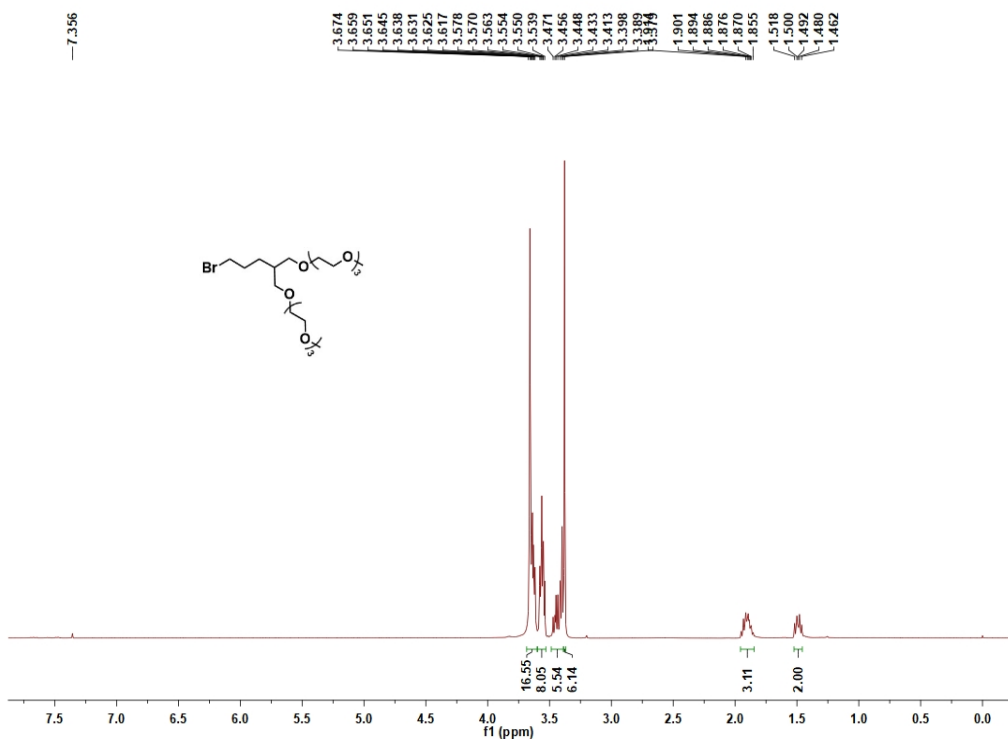


Fig. S11 ^1H NMR spectrum of compound **R**

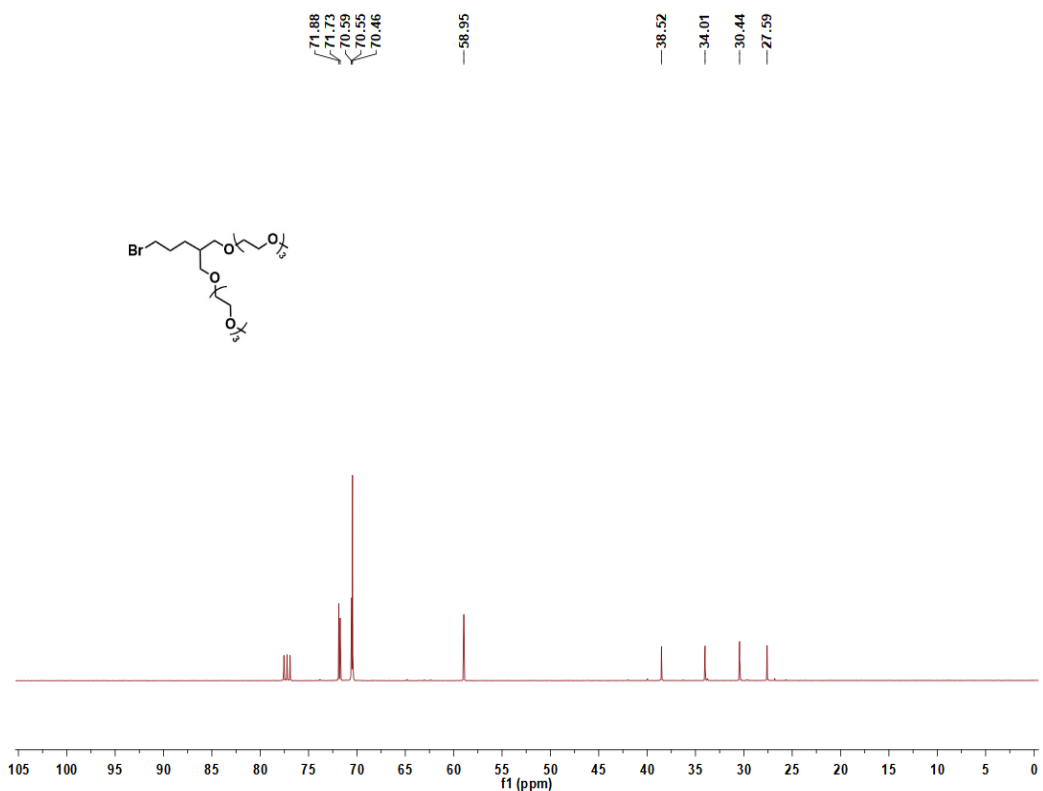


Fig. S12 ^{13}C NMR spectrum of compound **R**

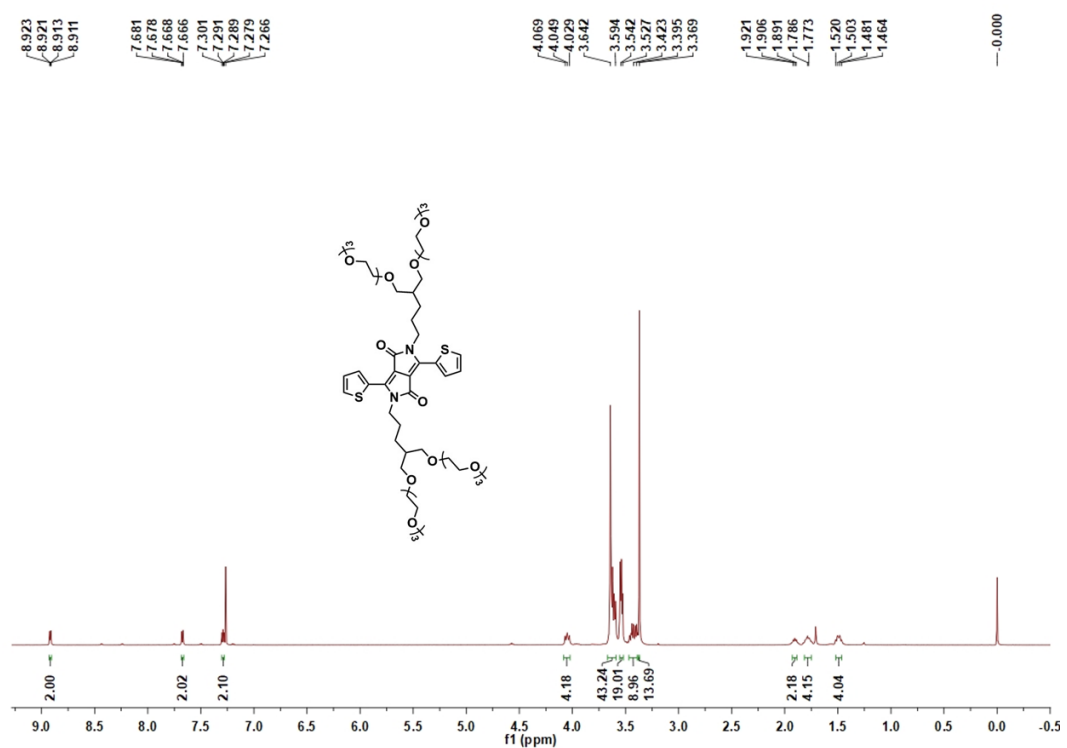


Fig. S13 ^1H NMR spectrum of compound 2

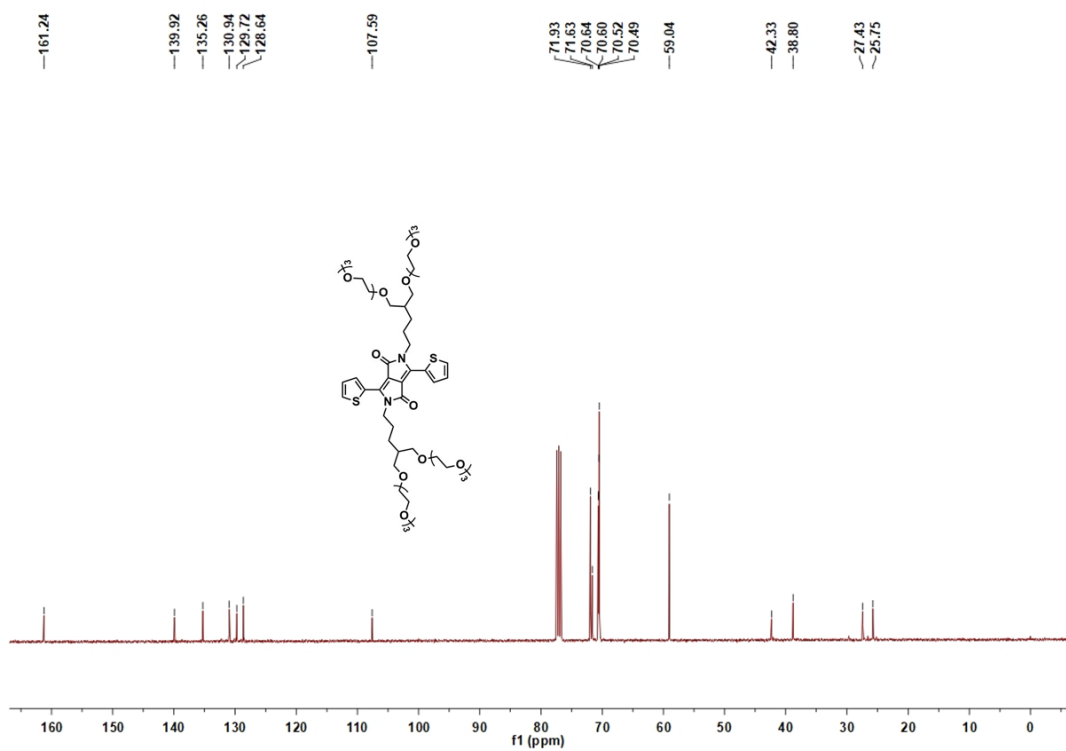


Fig. S14 ^{13}C NMR spectrum of compound 2

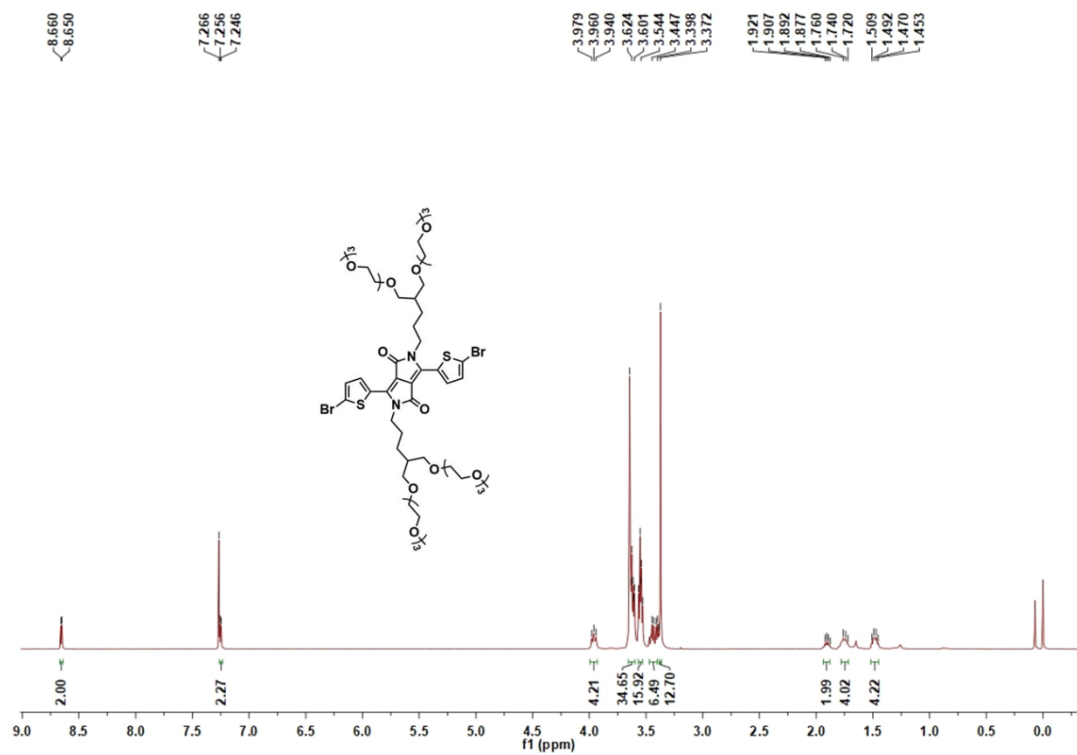


Fig. S15 ^1H NMR spectrum of compound 3

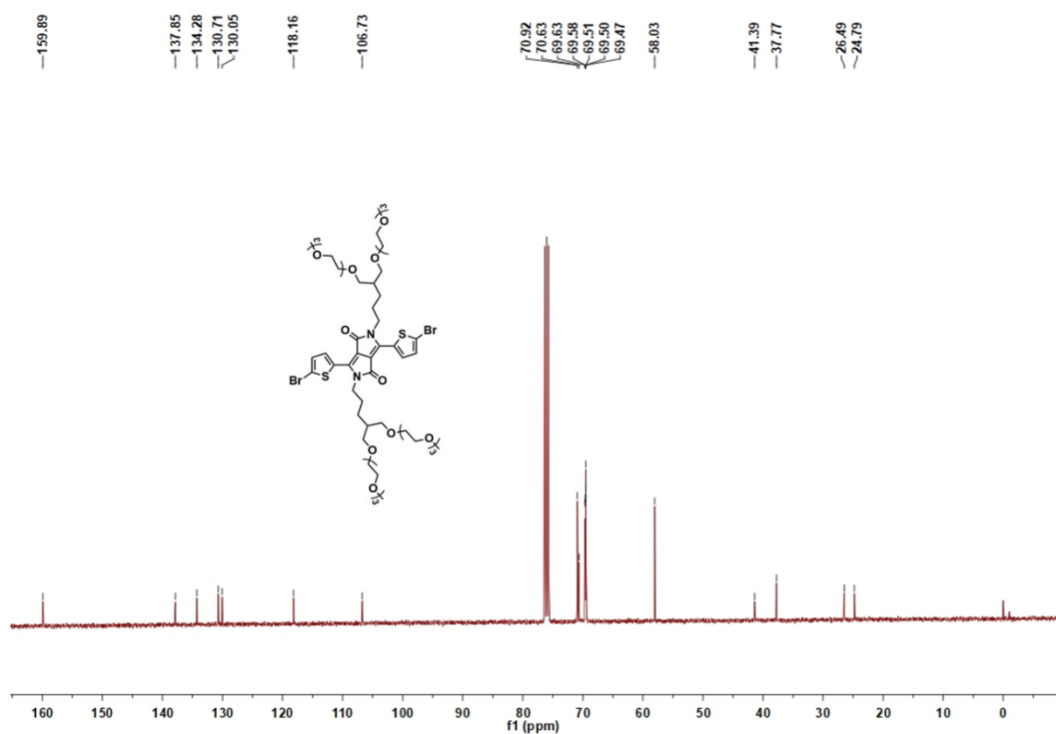


Fig. S16 ^{13}C NMR spectrum of compound 3

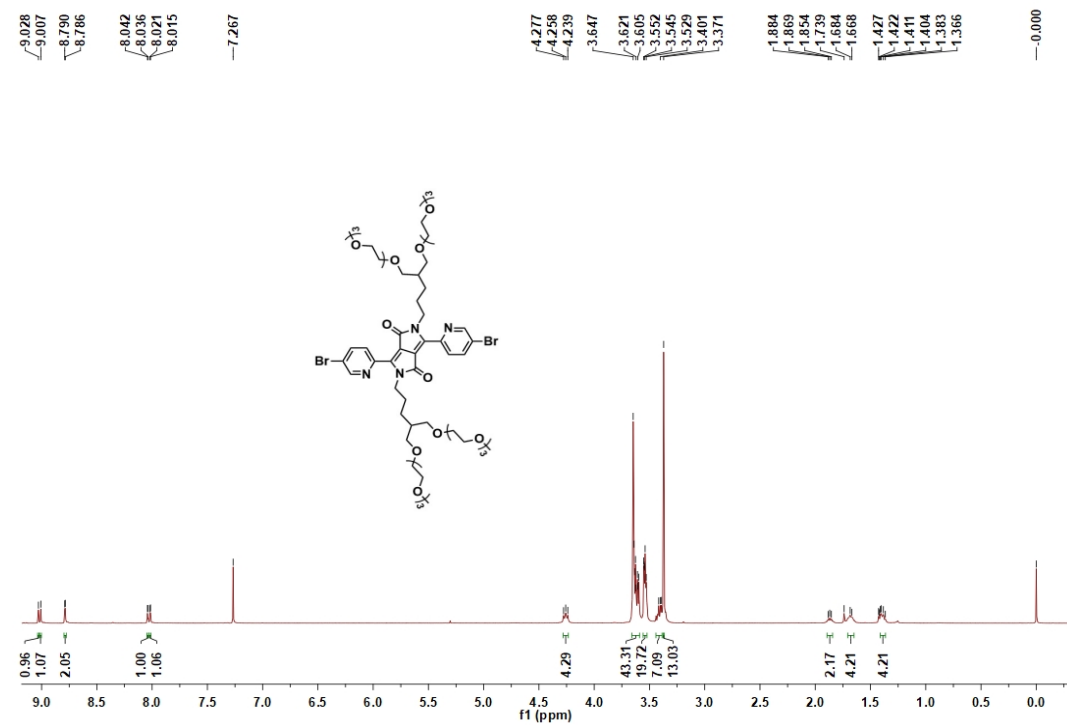


Fig. S17 ^1H NMR spectrum of compound gPyDPP

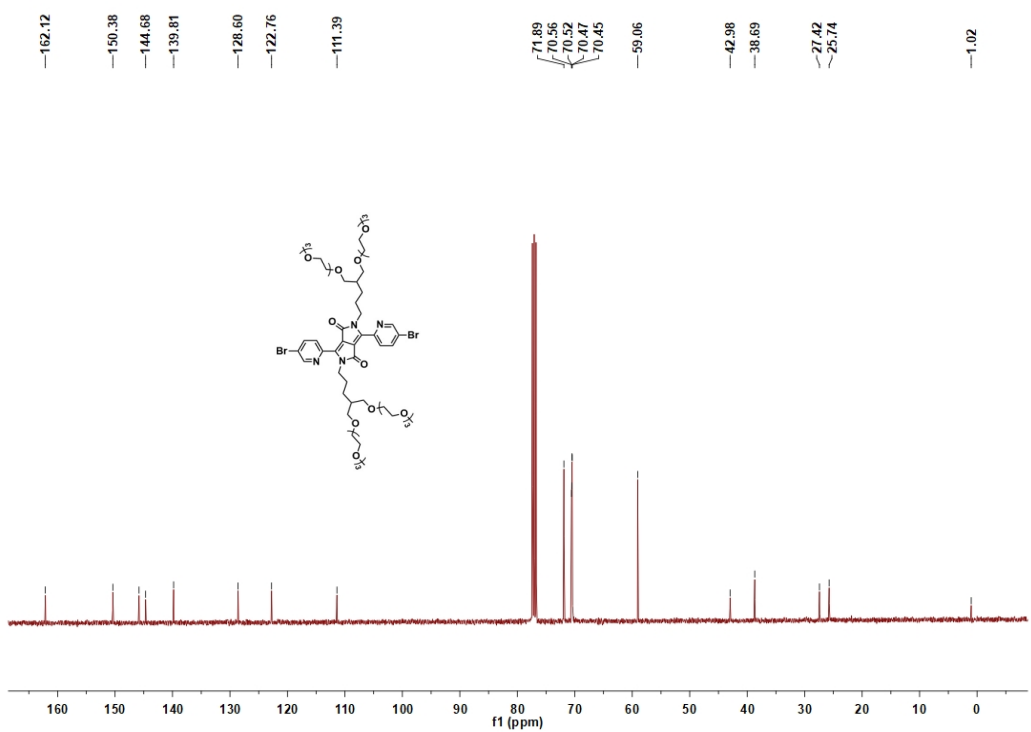


Fig. S18 ^{13}C NMR spectrum of compound **gPyDPP**

References

1. Frisch MJ, *et al.* Gaussian 16 rev. C.01. Wallingford, CT %! Gaussian 16; 2016.
2. GaussView V, Roy Dennington, Todd A. Keith, and John M. Millam, Semichem Inc., Shawnee Mission, KS, 2016.
3. Lu T, Chen F. Multiwfn: A multifunctional wavefunction analyzer. *J. Comput. Chem.* **33**, 580-592 (2012).
4. Humphrey W, Dalke A, Schulten K. Vmd: Visual molecular dynamics. *J Mol Graph* **14**, 33-38, 27-38 (1996).
5. Ohayon D, *et al.* Influence of side chains on the n-type organic electrochemical transistor performance. *ACS Appl. Mater. Interfaces* **13**, 4253-4266 (2021).
6. Wu HY, *et al.* Influence of molecular weight on the organic electrochemical transistor performance of ladder-type conjugated polymers. *Adv. Mater.* **34**, e2106235 (2022).
7. Feng K, *et al.* Fused bithiophene imide dimer-based n-type polymers for high-performance organic electrochemical transistors. *Angew. Chem. Int. Ed.* **60**, 24198-24205 (2021).
8. Wang YZ, *et al.* Green synthesis of lactone-based conjugated polymers for n-type organic electrochemical transistors. *Adv. Funct. Mater.* **32**, 2111439 (2022).
9. Shi JW, *et al.* Revealing the role of polaron distribution on the performance of n-type organic electrochemical transistors. *Chem. Mater.* **34**, 864-872 (2022).
10. Marks A, *et al.* Synthetic nuances to maximize n-type organic electrochemical transistor and thermoelectric performance in fused lactam polymers. *J. Am. Chem. Soc.* **144**, 4642-4656 (2022).
11. Feng K, *et al.* Cyano-functionalized n-type polymer with high electron mobility for high-performance organic electrochemical transistors. *Adv. Mater.*, 10.1002/adma.202201340, e2201340 (2022).
12. Jia H, *et al.* Engineering donor–acceptor conjugated polymers for high-performance and fast-response organic electrochemical transistors. *J. Mater. Chem. C* **9**, 4927-4934 (2021).